

## REQUIRED BASE SHEAR FOR REINFORCED CONCRETE BUILDINGS BASED ON EQUIVALENT LINEARIZATION METHOD

Eiichi Inai<sup>1</sup>, Hisahiro Hiraishi<sup>2</sup> and Kozue Kitamura<sup>3</sup>

<sup>1</sup> Professor, Graduate School of Science and Engineering, Yamaguchi University, Yamaguchi, Japan

<sup>2</sup> Professor, Dept. of Architecture, School of Science and Technology, Meiji University, Kanagawa, Japan

<sup>3</sup> Graduate Student, Graduate School of Science and Engineering, Yamaguchi University, Yamaguchi, Japan

Email: inai@yamaguchi-u.ac.jp, hiraishi@isc.meiji.ac.jp, m004vm@yamaguchi-u.ac.jp

### ABSTRACT :

This paper describes relationships between the required base shear and the allowable horizontal drift of reinforced concrete buildings based on the equivalent linearization method, where hysteretic damping of the degrading tri-linear restoring force characteristics model and asymmetry of response to ground motions are taken into consideration. These relationships can be expressed by simple equations and show excellent agreement with the results of time history response analyses.

**KEYWORDS:** Required base shear, Allowable horizontal drift, Equivalent linearization method

### 1. INTRODUCTION

The equivalent linearization method has been used in determining the required base shear of buildings since 2000 in Japan. However, the current method for evaluating the equivalent damping of reinforced concrete buildings is based on a degrading bi-linear restoring force characteristics model, which ignores hysteretic damping occurring after crack of concrete before yielding. The equivalent period is also evaluated on the assumption of the symmetric steady state response to ground motions though the asymmetry of response is often observed in the time history response analyses.

In this paper, time history response analyses of a single degree of freedom system with two degrading tri-linear restoring force characteristics models were conducted. The analytical results were compared with the predictions by the current equivalent linearization method. As a result, it is shown that the current method is not enough to predict the response. Then, based on the equivalent linearization method taking hysteretic damping of the degrading tri-linear restoring force characteristics model and the asymmetry of response into consideration, simple equations for relationships between the required base shear and the allowable horizontal drift of reinforced concrete buildings are presented. The predictions by the proposed equations show excellent agreement with the analytical results. Furthermore, this paper presents a method for evaluating the asymmetry of response, which is obtained from the assumption of the asymmetric steady state response to ground motions.

### 2. TIME HISTORY RESPONSE ANALYSIS

#### 2.1. Analytical Model

Figure 1 shows a single degree of freedom system used in the analyses, where  $Me$  is an effective mass of the building,  $H$  is an effective height of the building,  $R$  is a whole drift angle of the building, and  $\delta$  is a horizontal drift and equal to  $R \times H$ . Figure 2 shows a degrading tri-linear restoring force characteristics model used in the analyses, where  $Q$  is the base shear,  $Q_y$  is the yield strength,  $\delta_y$  is the yield deformation,  $K_y$  is the stiffness at yielding ( $=Q_y/\delta_y$ ),  $\lambda$  is the ratio of the crack strength to  $Q_y$ ,  $\alpha_y$  is the ratio of  $K_y$  to the elastic stiffness,  $\beta$  is the ratio of the stiffness after yielding to  $K_y$ ,  $\mu$  is the displacement ductility factor ( $=\delta/\delta_y$ ), and  $\eta$  is the index that represents the reduction of unloading stiffness. Takeda's hysteresis rule [Takeda et al. (1970)] is applied to the model.

As shown in Table 1, the parameters in the analyses are the height of the building  $H_T$  of 9 m, 21 m and 45 m,

the base shear coefficient  $C_B (=Q_y/(Me \times g)$ ,  $g$  is the gravity acceleration) of 0.2 - 1.2, and the amount of hysteretic damping after the crack point. Model A with  $\alpha_y$  of 0.5 and  $\lambda$  of 0.2 has smaller hysteretic damping than Model B with  $\alpha_y$  of 0.2 and  $\lambda$  of 0.5. The yield deformation is given by  $R_y \times H$ , where  $R_y$  is the whole drift angle at yielding and assumed to be 1/150, and  $H$  is assumed to be  $0.715H_T$  [Hiraishi et al. (2007a)].  $\beta$  and  $\eta$  are common factors in the analyses, and are 0.02 and 0.4 respectively. It should be noted that the instantaneous stiffness proportional viscous damping of 3% in the elastic range was used in the time history response analyses.

Twenty-five acceleration records with a target acceleration response spectrum and various random phases were generated as input ground motion in the analyses. The duration time of the records is 120 s. Figure 3 shows the acceleration response spectra (5% damping) of twenty-five records compared with the target acceleration spectrum  $S_a$  given by Eq. 2.2.1, where  $T$  is the natural period,  $A (=12 \text{ m/s}^2)$  is the acceleration in the response acceleration constant region, and  $T_c (=0.96 \text{ s})$  is the period at the boundary of the response acceleration constant region and the response velocity constant region. This target spectrum is the design spectrum in the second soil condition at the areas with seismic zone coefficient of 1.0, which is prescribed in Japanese seismic code. An example of the records is shown in Fig. 4.

$$S_a = \begin{cases} A \cdot \left( 0.4 + \frac{0.6}{0.16} T \right) & \text{for } T < 0.16 \text{ s} \\ A & \text{for } 0.16 \text{ s} \cong T < T_c \\ \frac{A \cdot T_c}{T} & \text{for } T_c \cong T \end{cases} \quad (2.1.1)$$

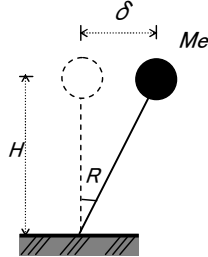


Figure 1 SDOF system

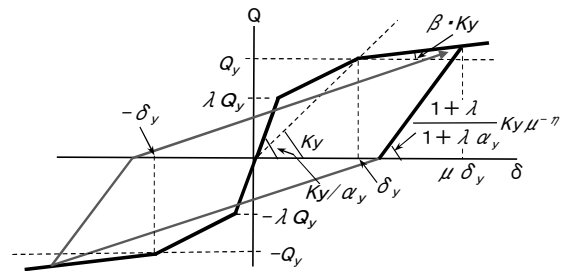


Figure 2 Hysteresis model

Table 1 Parameters in the analyses

$H_T$	9m	21m	45m	
$C_B = Q_y / (Me \cdot g)$	0.2	0.3	0.4	0.5
	0.6	0.7	0.8	1
	1.2			
$\alpha_y$	ModelA		ModelB	
	0.5		0.2	
$\lambda$	0.2		0.5	
common factors	$\delta_y = R_y \cdot H$ ( $H = 0.715H_T$ , $R_y = 1/150$ )			
	$\beta = 0.02$			
	$\eta = 0.4$			

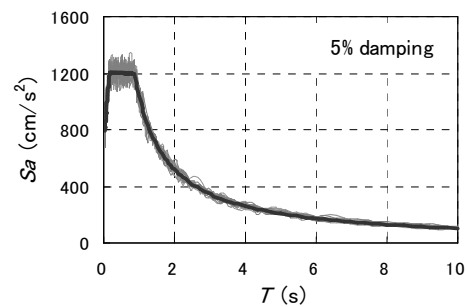


Figure 3 Acceleration response spectra

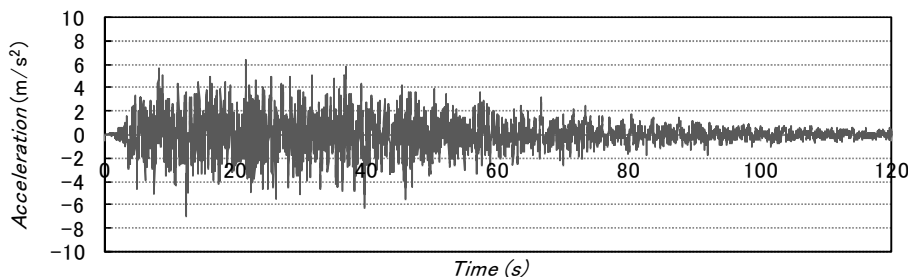


Figure 4 Example of input ground motion

**2.2 Comparison of the analytical results and the predictions by current equivalent linearization method**

Examples of base shear coefficient  $C_B$  – ductility factor  $\mu$  relationships obtained from the time history response analyses are shown in Fig. 5. Figure 6 shows comparisons of the analytical results and the predictions, where symbols of  $\circ$ ,  $\triangle$  and  $\square$  represent the average maximum response ductility factor in the responses to 25 records, and solid lines represent the predictions obtained from the current equivalent linearization method described in the following equations [Hiraishi et al. (2007a), Hiraishi et al. (2007b)];

$$C_B = \begin{cases} \frac{A}{g} \cdot F_h & \text{for the response acceleration constant region} \\ \frac{A \cdot T_c}{g \cdot T_d} \cdot \frac{F_h^2}{\mu} & \text{for the response velocity constant region} \end{cases} \quad (2.2.1)$$

where  $T_d$  is the period when the response displacement reaches the yield deformation  $\delta_y$  ( $=R_y \times H$ ) and is given by Eq. 2.2.2, and  $F_h$  is the reduction coefficient of the response acceleration due to the damping and is given by Eq. 2.2.3.  $he$  in Eq. 2.2.3 is the equivalent damping factor and is given by Eq. 2.2.4. Equations 2.2.3 and 2.2.4 are prescribed in Japanese seismic code. Equation 2.2.4 has been determined based on the hysteretic damping of the degrading bi-linear restoring force characteristics model.

$$T_d = \frac{(2\pi)^2}{A \cdot T_c} \cdot R_y \cdot H \quad (2.2.2)$$

$$F_h = \frac{1.5}{1 + 10he} \quad (2.2.3)$$

$$he = 0.25 \left(1 - \frac{1}{\sqrt{\mu}}\right) + 0.05 \quad (2.2.4)$$

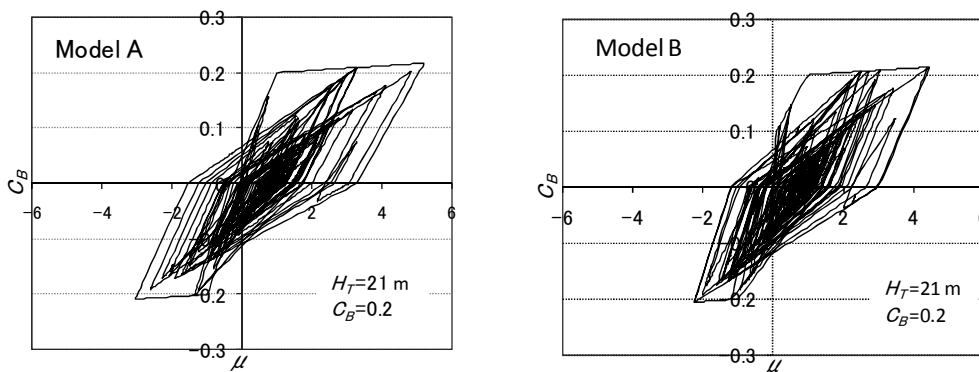


Figure 5 Examples of  $C_B$  –  $\mu$  relationships obtained from time history response analyses

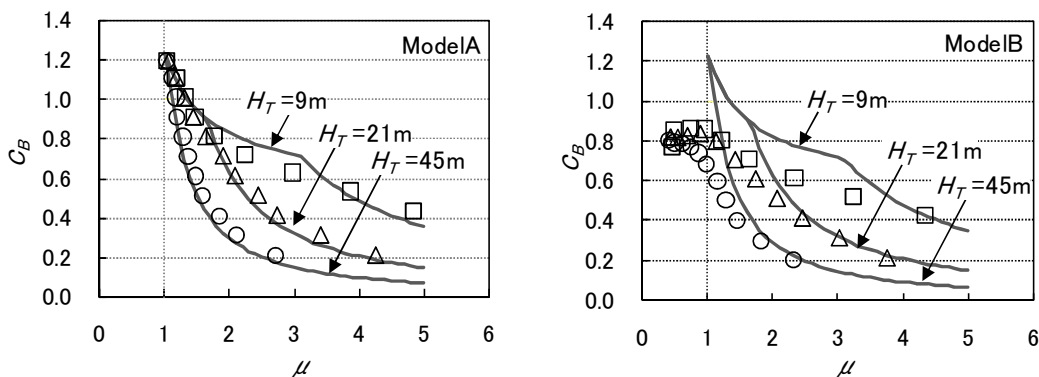


Figure 6 Comparisons of the analytical results and the predictions by the current equivalent linearization method

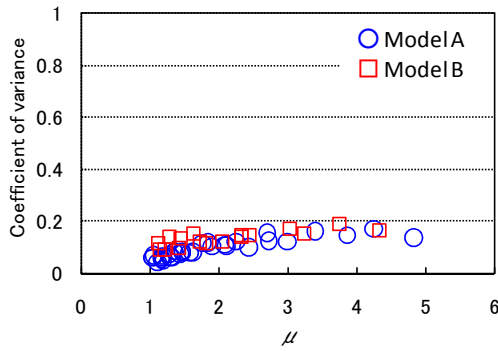


Figure 7 Relationship between coefficient of variance and  $\mu$

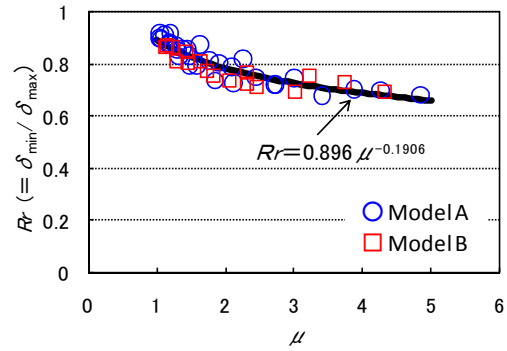


Figure 8 Relationship between  $Rr$  and  $\mu$

In Fig. 6, large differences between the analytical results and the predictions can be observed in case of Model B. This indicates that Eq. 2.2.4 does not give proper equivalent damping for the degrading tri-linear restoring force characteristics models such as Model B.

Figure 7 shows a relationship between the coefficient of variance of the maximum response ductility factor in the responses to 25 records and the average maximum response ductility factor  $\mu$ . However there is a tendency that the coefficient of variance becomes larger as  $\mu$  increases, the maximum value of the coefficient of variance is less than 0.2.

Figure 8 shows a relationship between  $Rr$  and the average maximum response ductility factor  $\mu$ , where  $Rr$  represents the average ratio of  $\delta_{min}$  to  $\delta_{max}$  in the responses to 25 records,  $\delta_{max}$  is the maximum response displacement, and  $\delta_{min}$  is the minimum response displacement (= the maximum response displacement at the opposite side). This relationship can be expressed by Eq. 2.2.5 approximately. As shown in Fig. 8, the asymmetry of response exists in the results of the time history response analyses.

$$Rr = 0.896 \cdot \mu^{-0.1906} \quad (2.2.5)$$

### 3. EQUIVALENT LINEARIZATION METHOD TAKING THE HYSTERETIC DAMPING OF DEGRADING TRI-LINEAR MODEL AND THE ASYMMETRY OF RESPONSE INTO CONSIDERATION

#### 3.1. Equivalent damping and Equivalent stiffness

Figure 9 shows comparison of the symmetric steady state response with an amplitude of the maximum displacement  $\delta_{max}$  and the asymmetric steady state response with  $\delta_{max}$  in the positive direction and  $\delta_{min}$  ( $= Rr \times \delta_{max}$ ) in the negative direction, where  $\Delta Wr$  and  $Ke$  represent the hysteresis area and the equivalent stiffness respectively in the symmetric steady state response condition,  $\Delta Wr^*$  and  $Ke^*$  represent the hysteresis area and the equivalent stiffness respectively in the asymmetric steady state response condition. The equivalent damping factor  $he^*$  in the asymmetric steady state response condition can be expressed by Eq. 3.1.1;

$$he^* = he,r^* + he,n^* \quad (3.1.1)$$

where  $he,r^*$  is the equivalent damping factor due to the hysteretic damping of the restoring force characteristics model, and  $he,n^*$  is the equivalent damping factor due to the instantaneous stiffness proportional viscous damping.  $he,r^*$  and  $he,n^*$  are expressed by Eq. 3.1.2 and Eq. 3.1.3 respectively, where  $he,r$  and  $he,n$  are given by Eq. 3.1.4 and Eq. 3.1.5 respectively.

$$he,r^* = \frac{1}{4\pi} \cdot \frac{\Delta Wr^*}{1/2 \cdot Ke \cdot \delta_{max}^2} = \frac{\Delta Wr^*}{\Delta Wr} \cdot he,r \quad (3.1.2)$$

$$he,n^* = \left( \frac{Ke^*}{Ke} \right)^{1.5} \cdot \left( \frac{1+Rr}{2} \right)^2 \cdot he,n \quad (3.1.3)$$

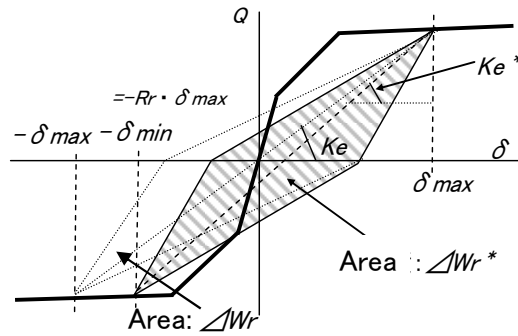


Figure 9 Comparison of symmetric steady state response and asymmetric steady state response

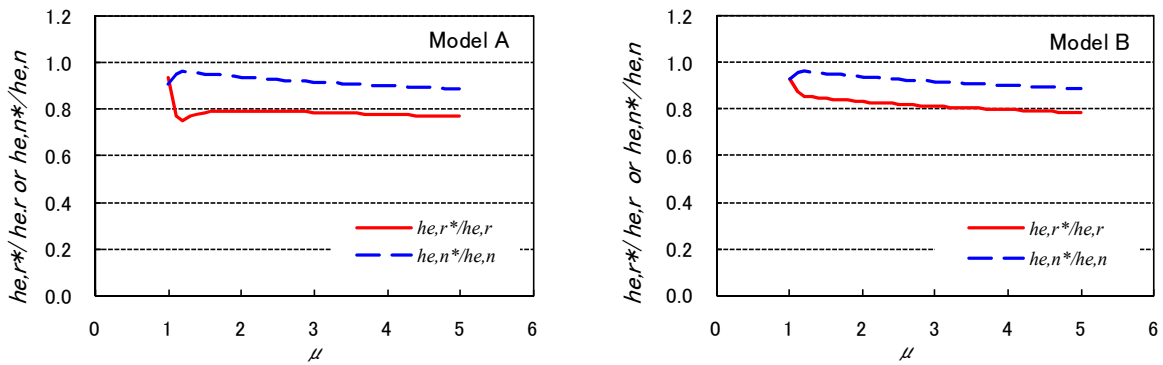


Figure 10 Relationships between  $he,r^*/he,r$  or  $he,n^*/he,n$  and  $\mu$

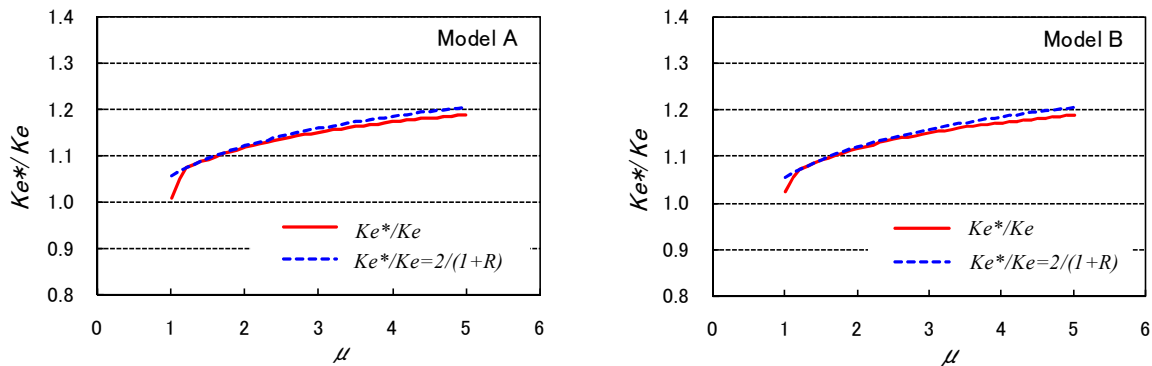


Figure 11 Relationships between  $Ke^*/Ke$  and  $\mu$

In case of the symmetric steady state response condition, the equivalent damping factor due to the hysteretic damping  $he,r$  is expressed by Eq.3.1.4, based on Takeda's hysteresis rule. The equivalent damping factor due to the instantaneous stiffness proportional viscous damping  $he,n$  is expressed by the Eq. 3.1.5, where  $hn$  is the viscous damping factor in the elastic range.

$$he,r = \frac{1}{\pi} \left[ 1 - \frac{\alpha_y + 1/\lambda}{1 + 1/\lambda} \{1 + \beta(\mu - 1)\} \cdot \mu^{(\eta-1)} \right] \quad (3.1.4)$$

$$he,n = \sqrt{\alpha_y} \cdot \sqrt{\frac{1 + \beta(\mu - 1)}{\mu}} \cdot hn \quad (3.1.5)$$

Using  $Rr$  of Eq.2.2.5,  $\Delta Wr^*$ ,  $Ke^*$ ,  $he,r^*$  and  $he,n^*$  can be calculated by following the restoring force characteristics model. Figure 10 shows relationships between  $he,r^*/he,r$  or  $he,n^*/he,n$  and  $\mu$ . The value of  $he,r^*/he,r$  is approximately 0.8. Figure 11 shows relationships between  $Ke^*/Ke$  and  $\mu$ . The value of  $Ke^*/Ke$  can be expressed by  $2/(1+Rr)$  approximately. Therefore, the following equations can be obtained.

$$he_{,r^*} = 0.8 \cdot he_{,r} \quad (3.1.6)$$

$$he_{,n^*} = \sqrt{\frac{1+Rr}{2}} \cdot he_{,n} \quad (3.1.7)$$

$$\frac{Ke^*}{Ke} = \frac{2}{1+Rr} \quad (3.1.8)$$

### 3.2 Comparison of the analytical results and the predictions by the equivalent linearization method taking the hysteretic damping of degrading tri-linear model and the asymmetry of response into consideration

The increase of the equivalent stiffness leads to the decrease of the equivalent period. The decrease of the period causes the decrease of the required base shear in the response acceleration constant region. Therefore, Eq. 2.2.1 that represents the required base shear coefficient is modified in the following form.

$$C_B = \begin{cases} \frac{A}{g} \cdot F_h \cdot \frac{Ke}{Ke^*} & \text{for the response acceleration constant region} \\ \frac{A \cdot T_c}{g \cdot T_d} \cdot \frac{F_h^2}{\mu} & \text{for the response velocity constant region} \end{cases} \quad (3.2.1)$$

Comparisons of the analytical results and the predictions by Eq. 3.2.1 are shown in Fig. 12, where  $he^*$  given by Eq. 3.1.1 has been used as  $he$  in Eq. 2.2.3, and Eq. 2.2.5, Eq. 3.1.6, Eq. 3.1.7 and Eq. 3.1.8 have been also used. In both Model A and Model B,  $C_B - \mu$  relationships given by Eq. 3.2.1 show excellent agreement with the analytical results.

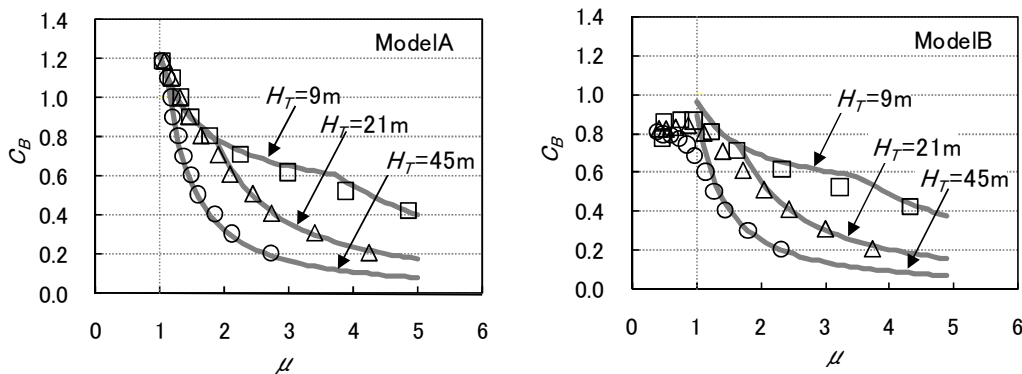


Figure 12 Comparisons of the analytical results and the predictions by Eq.3.2.1

## 4. EVALUATION OF THE ASYMMETRY OF RESPONSE

### 4.1. Assumed process to the asymmetric steady state response

The simplified degrading bi-linear restoring force characteristics model as shown in Fig. 13, where  $\xi$  is given by Eq. 4.1.1, is used for considering the asymmetry of response. Figure 14 shows the assumed process that the response to input ground motion reach the asymmetric steady state response, where  $\mu_{p,i}$  and  $\mu_{m,i}$  ( $i=1, 2, 3$ ) are the ductility factors at the peaks in the positive and negative directions respectively. At each response state in Fig. 14, Eq. 4.1.2 can be obtained from the assumption that area B in the negative direction is equal to area A in the positive direction.  $Rr$  is given by Eq. 4.1.3.

$$\xi = \frac{1+\lambda}{1+\lambda \cdot \alpha_y} \quad (4.1.1)$$

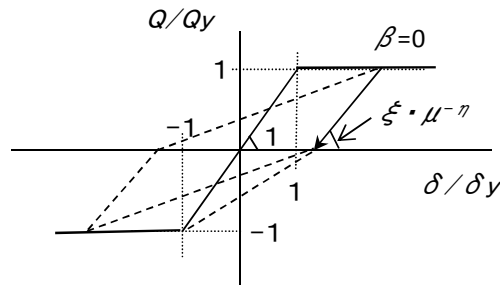


Figure 13 Simplified degrading bi-linear restoring force characteristics model

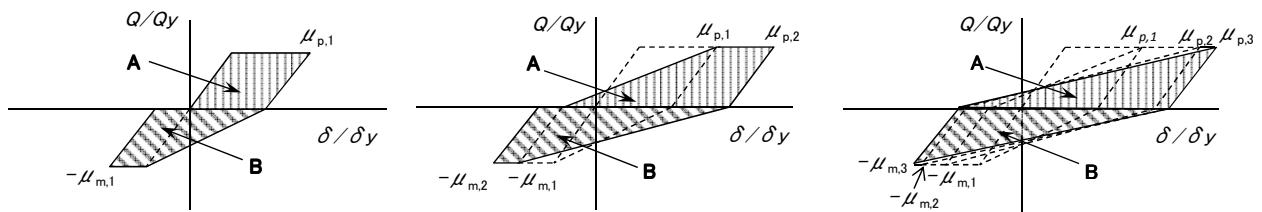


Figure 14 Assumed process to asymmetric steady state response

$$\mu_{m,i} - \frac{1}{2\xi} \mu_{m,i}^\eta = \frac{1}{2} \mu_{p,i} \quad \text{for } i=1, 2, 3 \quad (4.1.2)$$

$$Rr = \frac{\mu_{m,i}}{\mu_{p,i}} \quad (4.1.3)$$

#### 4.2. Comparison of the analytical results and the proposed equation

Figure 15 shows comparisons of the analytical results shown in Fig. 8 and Eq. 4.1.2. Equation 4.1.2 gives good agreement with the analytical results. For examining the effect of  $\eta$  in Eq. 4.1.2 on  $Rr$ , additional time history response analyses were conducted. The parameters in the analyses are  $H_T$  of 21 m,  $C_B$  of 0.2 - 1.2, and  $\eta$  of 0 and 0.9. The used restoring force characteristics model is identical to Model A except for the value of  $\eta$ . Examples of base shear coefficient  $C_B$  – ductility factor  $\mu$  relationships obtained from the analyses are shown in Fig. 16. Figure 17 shows comparisons of the average ratio of  $\delta_{min}$  to  $\delta_{max}$  in the responses to 25 records and Eq. 4.1.2. Equation 4.1.2 gives also good agreement with these analytical results.

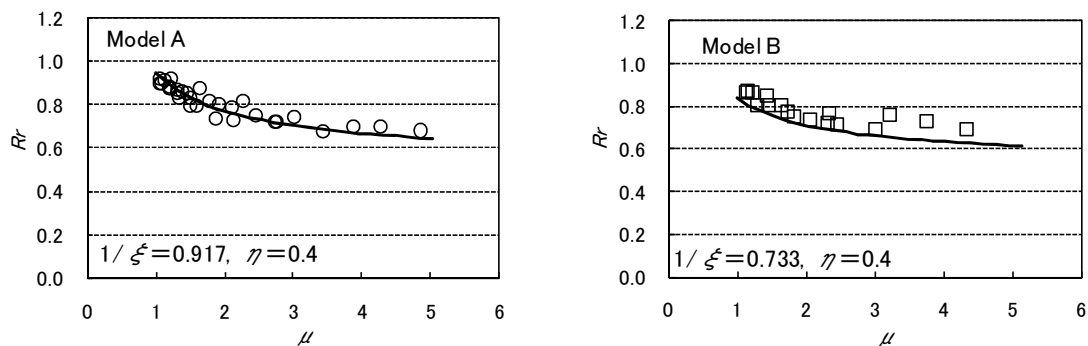


Figure 15 Comparisons of the analytical results and Eq. 4.1.2

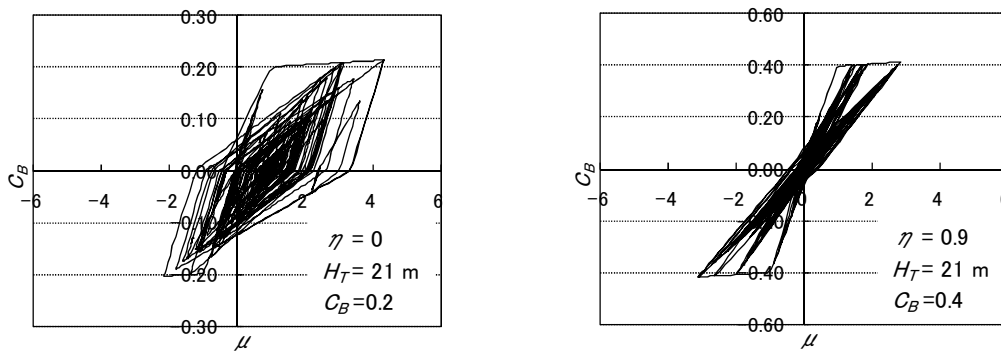


Figure 16 Examples of  $C_B$ - $\mu$  relationships obtained from time history response analyses

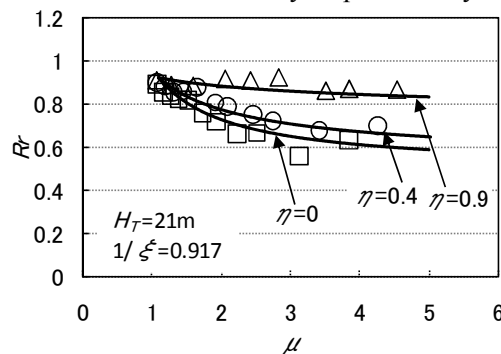


Figure 17 Comparisons of the analytical results and Eq. 4.1.2

## 5. CONCLUSIONS

The following conclusions can be drawn from this study.

- (1) The predictions of the maximum response to ground motions by the current equivalent linearization method have differences from the results of the time history response analyses. The reason for the differences is that the current method for the equivalent damping factor ignores hysteretic damping occurring after crack of concrete before yielding, and that the equivalent stiffness is evaluated on the assumption of the symmetric steady state response to ground motions.
- (2) Simple equations [Eq. 3.2.1] for relationships between the required base shear coefficient and the allowable horizontal drift of reinforced concrete buildings are presented based on the equivalent linearization method taking the hysteretic damping of the degrading tri-linear restoring force characteristics model and the asymmetry of response into consideration. The predictions by the proposed equations showed excellent agreement with the analytical results. However, the coefficient of variance of 20 % should be considered in the prediction.
- (3) The asymmetry of response can be approximately expressed by Eq. 4.1.2 which is obtained on the assumption of the asymmetric steady state response to ground motions.

## REFERENCES

- Takeda, T., Sozen, A.M., Nielsen, N.N. (1970). Reinforced concrete response to simulated earthquake. *Journal of the Structural Division, ASCE* **96:12**, 2557-2573.
- Hiraishi, H., Inai, E., Wada, T., Fukushima, T. (2007a). Evaluation of earthquake response and seismic performance of reinforced concrete buildings. *Journal of structural and construction engineering, AIJ* **613**, 105-112.
- Hiraishi, H., Inai, E., Fukushima, T. (2007b). Discussion of meaning of regulations and their rationalization of seismic code for reinforced concrete buildings. *Journal of structural and construction engineering, AIJ* **622**, 163-168.